Asymptotic Behavior of
Multivariable and Optimal System Designs

Ssu-Kei Wang, Mark Nagurka, Thomas Kurfess

EDRC 24-79-92

Asymptotic Behavior of Multivariable and Optimal System Designs

S. K. Wang, M. L. Nagurka, T. R. Kurfess

Department of Mechanical Engineering
Carnegie Mellon University
Pittsburgh, Pennsylvania 15213

Abstract

In this report we investigate the high gain asymptotic behavior of multivariable root loci. The proposed method groups the unbounded root loci of a non-singular m-input/m-output system into several Butterworth patterns as the gain tends toward infinity. A geometric technique provides direct realization of these asymptotic Butterworth patterns. Since integer as well as non-integer orders of these patterns can be determined, the method can be used to identify undesirable design conditions. Finally, the proposed method is extended to linear quadratic regulator problems where optimal root loci are identified. Three examples are presented to illustrate the effectiveness of the approach.

Introduction

This **piper** presents a geometrically-based approach for evaluating the asymptotic unbounded root loci behavior of multivariable control systems, including the optimal root loci behavior of linear quadratic regulator problems. Available algorithms for asymptotic conditions are complicated and are applicable only under certain assumptions. For instance, the technique proposed by Kouvaritakis and Edmunds (1979) can be applied to systems with generic structure (integer order) only. Studies by Johnson and Grimble (1981), Sastry and Desoer (1983), and Owens (1984) consider the asymptotic unbounded root loci for strictly proper systems. These studies impose assumptions on the simple null structure (Sastry and Desoer, 1983) or equivalent conditions of generic structure (Owens, 1984) to ensure the integer order of the Butterworth pattern.

The proposed approach relaxes the assumption of the simple null structure and enables a non-integer order of the pattern to be determined. Since this non-integer order corresponds to poor design conditions (Owens, 1980 and 1984), the approach provides a convenient means to detect design suitability. The algorithm starts from the evaluation of two sets of high gain eigenvalues of the closed-loop system. By introducing special eigenvalue magnitude and angle plots, the root loci can be grouped into several Butterworth patterns and the parameters of the asymptotic structure can be determined.

It has been shown (Shaked, 1978; Thompson *et aL,* 1982) that the optimal root locus is a special case of the classical root locus. It follows that the proposed approach can be extended to determine the asymptotic behavior of optimal root loci. An iterative algorithm to determine the asymptotic behavior of optimal root loci has been proposed by Kouvaritakis (1981) and later modified by Keerthi and Fannin (1983). These algorithms are complicated numerical procedures that can be difficult to implement. In comparison, the proposed method provides a conceptually simple and computationally efficient solution strategy.

System Configuration

Consider the system described by the state-space equations

$$* = Ax + Bu \qquad (1)$$

$$y = Cx + Du \qquad (2)$$

where x is an n dimensional state vector, u is an m dimensional control vector, y is an m dimensional output vector, and A, B, C, and D are constant matrices with appropriate dimensions. The transfer function matrix of the system is

$$G(s) = C(sI - A)^{-1}B + D \tag{3}$$

where I denotes the identity matrix and G(s) is an mxm matrix assumed to be invertible. The system is embedded in a closed-loop negative feedback configuration with a forward transfer function matrix kl where k is a scalar gain parameter. Figure 1 shows the block diagram of the closed-loop system. The closed-loop poles are the eigenvalues of the closed-loop system matrix

$$Ad(k) = A - kB(I + kDy\hat{}C \tag{4}$$

Asymptotic Structure

For the closed-loop system described in Figure 1, some closed-loop poles approach finite transmission zeros and the remaining closed-loop poles approach infinity as k approaches infinity. The "infinite" closed-loop poles group into several Butterworth patterns of different orders. If we consider a proper system with D=0 in equation (2), the asymptotic structure of the Butterworth pattern, modified from (Owens, 1984), can be expressed as

$$Sjp(k) = otj + \%k^{1/v}i + e_{jp}(k) \quad , \quad j = 1.....r \; ; \; p \text{ » } l,...,qj \tag{5}$$

and

$$\underset{k->-}{Km} \; £jp(k) = 0 \tag{6}$$

where Sjp(k) is the p-th closed-loop pole in the j-th Butterworth pattern with the number of closed-loop poles in this pattern being qj and the number of Butterworth patterns being r, Tjp (p=l,...,qj) are the distinct qj-th roots of a non-zero complex number, Vj is the order of the pattern, and otj is the pivot of the asymptotes. The magnitude and the angle of T_{jp} are called the radius and the direction of the closed-loop pole, respectively.

In almost all cases occurring in practice, the orders, v/s, are strictly positive integers and the r and qj in equation (5) can be replaced by m and Vj, respectively (Owens, 1984). For these cases, there are m Butterworth patterns and the number of closed-loop poles in a pattern is the order, Vj. For systetas with non-integer orders, the Butterworth

patterns can **have orders equal** only **to the** arithmetic means of subsets of the integer structural **invariants (Owens, 1978,1980,1984)**

$$N\ «(ni,\ n2,...»n_m) \quad ,\quad ti\backslash\ £\ n2\wedge **\#\wedge n_m \qquad (*j)$$

with

$$\bar{\pounds}^{n}\, i\wedge n \qquad (8)$$

where the ni's are integers. The asymptotic structure of equation (5) will be used to find the asymptotic behavior of the multivariable root locus.

Methodology

We are interested in grouping the unbounded root loci into several Butterworth patterns and finding the parameters in these asymptotic structures.

Multivariable Root Loci

Eigenvalue Magnitude and Angle Hots

From equation (4), we first calculate the closed-loop poles for two large values of k, denoted by ki and k2 where ki > k2 » 1

$$\lambda_i^{(1)} = \text{eig}[A_{cl}(k_1)] \quad ,\quad i = 1,...,n$$

(9a-b)

$$\lambda_i^{(2)} = \text{eig}[A_{cl}(k_2)] \quad ,\quad i = 1,...,n$$

where the subscript i denotes the branch. These closed-loop poles can be portrayed in the eigenvalue magnitude **and angle** plots of Figure 2 that show the eigenvalue magnitude and angle, respectively, as a function of k.

Branch Order

From equations (5) and (6), 0Cj and $e_{jp}(k)$ are negligible when k approaches infinity. As a result, the unbounded high gain root locus in the same Butterworth pattern can be described by

$$Sjp(k) = T]jpk^{1/Vj} \quad ,\quad j = l,.-.,r\ ;\ p = l,...,qj \qquad (IQ)$$

Assuming ki and k_2 arc large enough to satisfy **the** asymptotic structure of equation (10), it can be shown **that**

$$X_i^{(1)}{}_1(k=)\eta_i l^M \quad , \quad i = l.\ldots.n$$

(lla-b)

$$\lambda_i^{(2)}(k_2) = \eta_i k_2^{1/v_i} \quad , \quad i = 1,\ldots,n$$

where Vi is the order of the i-th branch and T}, is the corresponding non-zero complex number which is constant in each branch. Taking the magnitude of equations (lla-b) yields

$$\mathbf{ft}' = \frac{|\lambda_i^{(1)}|}{ki^*} = \frac{|\lambda_i^{(2)}|}{kj^*} \tag{12}$$

which leads to

$$1 \wedge \frac{\log|\lambda_i^{(1)}| - \log|\lambda_i^{(2)}|}{\log ki - \log k2} \tag{13}$$

Vi

The order of each branch can be determined from equation (13) which represents the slope in the magnitude plot: If the slope of the magnitude plot is zero, equation (13) requires that $\wedge i^{(1)}$ and $\wedge i^{(2)}$ are in near proximity to each other indicating that the closed-loop pole approaches a finite transmission zero.

The exact order can be obtained directly when V; in equation (13) converges to an integer. When Vi converges to a non-integer real number, the order should be available from equations (7) and (8) since the Butterworth patterns have orders equal only to the arithmetic means of subsets of the integer structural invariants. If v_x does not converge to the arithmetic mean, it implies that the selected ki and k2 are not large enough to satisfy the asymptotic structure of equations (1 la-b) and larger ki and k2 are necessary.

Pattern **Family**

After the order of each branch is determined, the next step is to group the branches into several patterns. Considering equation (10), since the %'s are the distinct cy-th roots of a non-zero complex number, the magnitude of rjjp is a constant for those closed-loop poles in the same pattern. It follows that for a given k the closed-loop poles belonging to

the same pattern have die same order and magnitude implying an overlap in the magnitude plot This is the necessary condition for the family of a pattern.

Sometimes die necessary condition is not enough to group the patterns, as in the case of two second order patterns with the same radius. In this case, we need information about the angle of equation (10). Again using the fact that the Tljp's are the distinct qj-th roots of a non-zero complex number and the angle of Sjp is the same as the angle of TVjp the eigenvalues in the same pattern have the relation:

$$\Delta\theta \cong \angle\lambda^{\wedge} - \angle\lambda \tag{14}$$

where A6 is the adjacent angle of the asymptotes and the i-th and j-th branches belong to the same pattern. Because the adjacent angle of the asymptotes is a constant in a pattern, equation (14) can be used to determine the eigenvalues that belong to the same Butterworth pattern. Then, all the eigenvalues in equations (9a-b) can be grouped into several patterns as

$$s_{jp}^{\{1\}} = \text{eig}[A_c i(ki)] \quad > \quad j = 1.....T \; ; \; P = l,...,qj$$

(15a-b)

$$sj^{\wedge}eigCAc^{\wedge})] \quad , \quad k\,! > k_2 \gg l$$

When the orders are all integers, it can be verified that

$$r = m \tag{16}$$

$$dc = Vj \tag{17}$$

Pattern Pivot

Once the root loci in a pattern are known, the pivot of the asymptotes can be determined by calculating the location of the centroid of the high gain closed-loop poles in that pattern. Here the pivot is denoted by

$$aj = Xj + /Yj \tag{18}$$

where *i* is the square root of -1. The centroid location can be determined from

$$X_j = \frac{\sum_{p=1}^{q_j} \mathrm{Re}\left[s_{jp}^{(1)}\right]}{q_j} \tag{19}$$

$$Y_j = \frac{\sum_{p=1}^{q_j} \mathrm{Im}\left[s_{jp}^{(1)}\right]}{q_j} \tag{20}$$

Pattern Directions

From equation (10), the direction of Tjp is the same as the angle of Sjp. It follows that the direction can be read directly from the angle plot, *i.e.*,

$$\angle\eta_{jp} = \angle s_{jp}^{(1)}$$

A more precise solution is available using the asymptotic structure of equation (5). The direction can be determined by

$$\angle\eta_{jp} = \angle\left(s_{jp}^{(1)} - \alpha_j\right) \tag{22}$$

Pattern Radius

If we substitute the high gain ki, the corresponding closed-loop pole sjp[1]\ the order Vj, and the pivot otj into equation (5) and let £jp(ki)=O, the radius can be determined from

$$|\eta_{jp}| = \left|\text{''}\right]?\text{-«}fc^{IM} \tag{23}$$

It is worth noting that the pivot, direction, and radius are not exact since exact solutions are achieved only as ki approaches infinity. The accuracy depends on ki. In order to ensure the accuracy, we define the error of convergence:

$$\text{••*• } s\,£\,r^{Vi} \tag{24}$$

where

$$\text{slope} = \frac{\text{Io2ls}_{jp}^{(1)}\text{l-logls}^{(2)}\text{l}}{\text{Iogki-logk2}} \tag{25}$$

In practice, if the error of convergence is within a specified tolerance, then the accuracy can be guaranteed.

Optimal Root Loci

The optimal root loci represent the closed-loop poles of the linear quadratic regulator as fe control weighting in the performance index is varied Since the optimal root locus is a special case of the regular root locus, the proposed geometric technique can be used to compute the optimal asymptotic behavior.

Linear Quadratic Regulator

For the state-space system

$$* = Ax + Bu \tag{26}$$

$$y = {}^{c} * \tag{27}$$

where x is n dimensional, and u and y arc m dimensional, the objective is to determine an optimal control trajectory

$$u = -K_c x \tag{28}$$

that minimizes the cost function

$$J = \int_{J0} (yTQy + pu^{r}Ru)dt \tag{29}$$

where $Q = Q^{r} \geq 0$ and $R = R^{r} > 0$ arc weighting matrices and p is a scalar. Assuming that (A,B) is stabilizable and (C,A) is detectable, the solution for Kc can be determined by solving the algebraic Riccati equation. Substituting equation (28) into (26) gives the closed-loop system matrix of the linear quadratic regulator as

$$A_c i(p) = A - BKc(p) \tag{30}$$

Its eigenvalues, the closed-loop poles, are functions of p. As p varies from infinity to zero, the closed-loop poles trace out an optimal root locus.

Asymptotic Structure

When p approaches zero, some closed-loop poles approach finite transmission zeros and the remaining closed-loop poles approach infinity. It has been proven (Kwakernaak, 1976) that those "infinite** closed-loop poles group into several Butterworth patterns of different orders. The asymptotic structure of the Butterworth pattern of order Vj can be expressed as

$$s_{jp}(1/\rho) = \eta_{jp}(1/\rho)^{1/v_j} + \varepsilon_{jp}(1/\rho) \quad , \quad j = 1,\ldots,m \; ; \; p = 1,\ldots,v_j \tag{31}$$

$$J \quad \varepsilon_{jp}(1/\rho) = O \tag{32}$$

where Vj is an even integer and % is the distinct Vj-th root of a real number. Compared to the asymptotic structure of multivariable root loci, equation (31) has the form of equation (5) with the pivot located at the origin and with k replaced by 1/p. Therefore, by denoting

$$1/p - k \tag{33}$$

the formula derived previously can be used to find the asymptotic optimal root loci.

Solution Procedure

The solution strategy follows the methodology of the multivariable case with minor modifications. For the calculations of eigenvalues in equations (9a-b), A^ can be obtained after solving the algebraic Riccati equation. An alternative method for finding these closed-loop poles is from the Hamiltonian matrix:

$$H = \begin{bmatrix} A & -\frac{1}{\rho} BR^{-1}B^T \\ -C^r QC & -A^T \end{bmatrix} \tag{34}$$

Its eigenvalues are symmetric about the imaginary axis and those in the left-half plane are the closed-loop poles (Thompson *et* a/., 1982).

From the angle plot, we may obtain the approximate solution for the direction (the exact solution can be obtained only when pi approaches zero.) However, it has been proven (Kouvaritakis, 1978,1981) that the asymptotes of the optimal root loci are arranged in the direction of the Vj-th roots of +1 that lie in the left half of the complex plane. Figure 3 shows the Butterworth configurations for Vj=2,4, 6, and 8 which indicate the directions of the asymptotes. Thus, the directions can be determined exactly from the order Vj and the angle plot provides a direct realization of these directions.

The solution procedure for finding the asymptotic structure of the optimal root loci is summarized as follows:

1. For two small values of p, calculate the closed-loop poles.
2. Plot the closed-loop poles as a function of 1/p in eigenvalue magnitude and angle plots.
3. Determine the order from the slope in the magnitude plot

4. Group **the** patterns by the overlaps of the closed-loop poles in the **iragnfandeptot**
5. **Dittrmincthedirectkms from the angle plot or using Figure 3.**
6. **Determine** the radii from equation (23) where k=l/p.
7. **Check die accuracy** from equation (24).

Examples

Example 1 investigates the asymptotic behavior of the multivariablc root locus. Aldiough the asymptotic structure of equation (5) is derived for proper systems, the results of example 1 show that it can also be applied to non-proper systems. Example 2 considers the asymptotic behavior of optimal root loci. Example 3 studies a non-integer order system.

Example 1

This example, adapted from Kouvaritakis and Edmunds (1979), considers a seventh-order system with the state-space form described in equations (1) and (2), where

$$\mathbf{A} = \frac{1}{16}\begin{bmatrix} -32 & -80 & 16 & 0 & 0 & 0 & 0 \\ 16 & -64 & -16 & 0 & 0 & 0 & 0 \\ 0 & 0 & 8 & 0 & 0 & 0 & 0 \\ 0 & 0 & 0 & -32 & -80 & 0 & 0 \\ 0 & 0 & 0 & 16 & -64 & 0 & 0 \\ 1653 & 0 & 0 & 3424 & 0 & -32 & -80 \\ 76 & 0 & 0 & 928 & 0 & 16 & -64 \end{bmatrix} \quad (35)$$

$$\mathbf{B} = \begin{bmatrix} 1 & 0 & 0 \\ -1 & 2 & -2 \\ 1 & 1 & 2 \\ 0 & 1 & 0 \\ 0 & 0 & 1 \\ 0 & 0 & 0 \\ 0 & 0 & 0 \end{bmatrix} \quad (36)$$

$$\mathbf{C} = \frac{1}{16}\begin{bmatrix} 8 & -16 & 0 & 0 & 0 & 0 & 0 \\ -8 & -8 & 16 & -15 & -37 & 8 & 0 \\ 0 & 8 & 16 & -68 & 36 & 0 & 8 \end{bmatrix} \quad (37)$$

$$\mathbf{D} = \begin{bmatrix} -8 & -2 & 10 \\ -4 & -1 & 5 \\ -8 & -2 & 10 \end{bmatrix} \quad (38)$$

Closed-loop poles were calculated at ki=10^7 and k_2=10^6. Table 1 lists the results and the corresponding eigenvalue magnitude and angle plots are shown in Figure 4. In the magnitude plot, the branches i=l to i=4 overlap and have the same slope of 1/2, indicating second order patterns. Because there are two branches in a second order pattern, the branches i=l to i=4 belong to two second order Butterworth patterns. Applying equation (14), the angle plot shows branches i=l and i=2 are in the same pattern since the angle difference is 180° and branches i=3 and i=4 are in the same pattern for the same reason. The branches i=5 to i=7 have zero slopes in the magnitude plot which imply bounded branches.

The pivots for these second order patterns were evaluated using equations (18)-(20) as

$$\text{cti} = 19.24\text{-}1' 11.87 = 22.61\text{Z-}31.67^0$$

$$a_2 = 19.24 + \text{i } 11.87 = 22.61\text{Z}31.67^0 \qquad (39a\sim b)$$

where cti denotes the pivot of branches i=l and i=2 and ct2 denotes the pivot of branches i=3 and i=4. Using equations (22) and (23) to calculate the directions and radii, the complete asymptotic structures are

$$\text{sn} = 22.61\text{Z-}31.67^0 + 1\text{O.OZ}63.44^0\ k^{1/2} \qquad \text{i=1()}$$

$$\text{S12} = 22.61\text{Z-}31.67^0 + 1\text{O.OZ}243.4^0\ k^{1/2} \qquad \text{(i=2)}$$

$$s_2\text{i} = 22.61\text{Z}31.67^0 + 1\text{O.OZ}296.6^0\ k^{1/2} \qquad \text{(i=3)} \qquad (40a\sim d)$$

$$s_2\text{2} = 22.61\text{Z}31.67^0 + 10.0\text{Z}116.6°\ k^{1/2} \qquad \text{(i=4)}$$

The error of convergence, calculated from equation (24),

$$\backslash i_n = \text{-}2.1\text{xKH}$$

$$\backslash i_n = 2.7\text{xl(H}$$

$$\text{M« -}2.1\text{X}10\text{-} \qquad (41a\text{-}d)$$

$$\text{H22} = 2.7\text{xl(H}$$

demonstrates high accuracy of the asymptotic structures. The pivots and the asymptote directions are the same as those computed by Kouvaritakis and Edmunds (1979).

Example 2

This example, adapted from Kwakemaak and Sivan (1972, example 3.21, pp. 293-297), considers the longitudinal dynamics of an aircraft model described by equations (26) and (27) with

$$A = \begin{bmatrix} -0.158 & 0.02633 & -9.81 & 0 \\ -0.1571 & -1.03 & 0 & 120.5 \\ 0 & 0 & 0 & 1 \\ 0.0005274 & -0.01652 & 0 & -1.466 \end{bmatrix} \quad (42)$$

$$B = \begin{bmatrix} 0.0006056 & 0 \\ 0 & -9.496 \\ 0 & 0 \\ 0 & -5.565 \end{bmatrix}, \quad C = \begin{bmatrix} 1 & 0 & 0 & 0 \\ 0 & 0 & 1 & 0 \end{bmatrix} \quad (43),(44)$$

It is to be controlled such that the cost function of equation (29) is minimized where

$$Q = \begin{bmatrix} 0.02 & 0 \\ 0 & 50 \end{bmatrix}, \quad R = \begin{bmatrix} 0.0004 & 0 \\ 0 & 2500 \end{bmatrix} \quad (45),(46)$$

Closed-loop poles were evaluated at $p_1=10^{7}$ and $p_2=10^{6}$. The results are listed in Table 2 and the corresponding eigenvalue magnitude and angle plots are shown in Figure 5. From the magnitude plot in Figure 5, the branches i=1 and i=2 coincide and have the same slope of 1/4. This means that these branches belong to a pattern with order four. The branch i=3 has a slope of 1/2 indicating a second order pattern. This order can also be found from equation (13). The branch i=4 has zero slope which implies that this branch approaches a finite zero. From the angle plot, the second order pattern has a direction of 180° and the fourth order pattern has directions of ±135°. These results can be verified by Figure 3 as Vj=2 and Vj=4. Using equation (23) to determine the radii, the asymptotic structures for the second and fourth orders can be obtained as

$$s_n \sim a_{004283} Z 180° p^{-1/2} \quad \text{(second order)} \quad (47)$$

$$S_{2p} \sim 4 | S_{871} Z \pm 135° p^{-1/4}, \quad p=1,2 \quad \text{(fourth order)} \quad (48)$$

which are approximate since p is finite. Again, the error of convergence from equation (24)

$$\mu_{11} = 6.9 \times 10^{-4}, \quad \text{(second order)} \quad (49)$$

$$|i_{2p} = 1.8 \times 10^{-5}, \quad p=1,2 \quad \text{(fourth order)} \quad (50)$$

shows that the radii are quite accurate. Equations (47) and (48) are in close agreement with the published results (Kwakernaak, 1976).

Figure 6 shows the complete eigenvalue magnitude and angle plots for this example. The dotted lines represent the closed-loop poles determined firom the Hamiltonian matrix. The magnitudes of the asymptotic structures are shown in the magnitude plot by the solid lines. The overlap of the dotted and solid lines for small p represents the asymptotic structure. The magnitude plot indicates that when p is smaller than 10^{-5}, the asymptotic structure can be used rather than solving for the eigenvalues of the Hamiltonian matrix to determine the closed-loop poles. The asymptotic structure is easily obtained from the proposed method and offers advantages in constructing the optimal root locus.

Example 3

This example considers a third order proper system with two inputs and two outputs. The state space model is described by equations (1) and (2) with

$$\mathbf{A}=\begin{bmatrix} 0 & 0 & 0 \\ 0 & 0 & 1 \\ 0 & 0 & 0 \end{bmatrix}, \quad \mathbf{B}=\begin{bmatrix} 0 & r \\ 0 & 0 \\ -1 & 0 \end{bmatrix}, \quad \mathbf{C}=\begin{bmatrix} 1 & 0 & 0 \\ 0 & 1 & 0 \end{bmatrix}, \quad \mathbf{D}=\begin{bmatrix} 0 & 0 \\ 0 & 0 \end{bmatrix} \qquad \textbf{(51)-(54)}$$

Closed-loop poles evaluated at $k_1=10^7$ and $k_2=10^6$ are listed in Table 3. The corresponding eigenvalue magnitude and angle plots are shown in Figure 7. From the magnitude plot, all of the branches overlap with a slope of 0.6667 and the order is 1.5. Since the order does not converge to an integer, we need to use the integer structural invariants to find the exact order. From equations (7) and (8), we have

$$\mathbf{N} = \{n_1, n_2\} \qquad \textbf{(55)}$$

and

$$n_1 + n_2 \leq 3 \qquad (56)$$

which leads to

$$N - \{1_f 2\} \qquad \textbf{(57)}$$

The arithmetic mean of N, 3/2, is the exact order which can be verified by the magnitude plot. Determining the pivot, directions, and radii from equations (18)-(23) gives the asymptotic structure:

$$s_{1p} = 1.0\angle(p-1)\cdot 120^\circ)k^{2/3} \quad . \quad P = \triangleright^2 > ^3 \qquad (58)$$

with an error of **convergence** less than $1(H^4$.

Conclusion

Solutkm procedures for determining asymptotic behavior of multivariablc root loci have been presented in the literature. These procedures involve complex numerical algorithms that are generally difficult to implement As an alternative, we propose a coherent geometrically-based approach for obtaining the asymptotic root locus behavior. The approach can handle general problems by relaxing the simple null assumption and can be used to detect unsatisfactory design conditions. Utilizing the eigenvalue magnitude and angle plots, the proposed method provides direct realization of the directions and radii of the asymptotic eigenvalue patterns. In summary, the proposed method is a suggested approach for generating asymptotic root loci, including optimal root loci.

References

Johnson, M. A. and Grimble M. J., 1981, "On the Asymptotic Root-Loci of Linear Multivariable Systems," International Journal of Control, Vol. 34, No. 2, pp. 295-314.

Keerthi, S. S. and Fannin, D.R., 1983, "Comments on and Modifications to 'On the Asymptotic Behaviour of Optimal Root Loci[1]," International Journal of Control, Vol. 37, No. 1, pp. 215-220.

Kouvaritakis, B., 1978, "The Optimal Root Loci of Linear Multivariable Systems," International Journal ftf CffilTftr, Vol. 28, No. 1, pp. 33-62.

Kouvaritakis, B., 1981, "On the Asymptotic Behaviour of Optimal Root Loci," International Journal of ChntroL, Vol. 33, No. 6, 1165-1170.

Kouvaritakis, B. and Edmunds, J. M., 1979, ''Multivariable Root Loci: A Unified Approach to Finite and Infinite Zeros," International Journal of Control, Vol. 29, No, 3, pp. 393-428.

Kwakernaak, R and Sivan, R., 1972, Linear Optimal Control Systems, Wiley-Interscience, New York.

Kwakernaak, H., 1976, "Asymptotic Root Loci of Multivariable Linear Optimal Regulators," IERR Transactions on Automatic Control, Vol. AC-21, pp. 378-382.

Owens, D. H., 1978, "On Structural Invariants and the Root-Loci of Linear Multivariable Systems," International Journal of Control, Vol. 28, No. 2, pp. 187-196.

Owens, D. H., 1980, "A Note on the Orders of the Infinite Zeros of Linear Multivariable System*,* International Journal of ControL Vol. 31, No. 2, pp. 409-412.

Owens, D. H* 1984, "On the Generic Structure of Multivariable Root-Loci," International Journal of Control, Vol. 39, No. 2, pp. 311-319.

Sastry, S. S. and Desoer, C. A., 1983, "Asymptotic Unbounded Root Loci- Formulas and Computation/[1] IKKK Transactions on Automatic ControL Vol. AC-28, pp. 557-568.

Shaked, U_M 1978, 'The Asymptotic Behavior of the Root-Loci of Multivariable Optimal Regulators," TRFK Transactions on Automatic ControL Vol. AC-23, pp. 425-430.

Thompson, P. M., Stein, G., and Laub, A. J., 1982, "Angles of Multivariable Root Loci," IRKR Transactions on Automatic ControL Vol. AC-27, pp. 1241-1243.

Table and Figure Captions

Table 1 Closed-Loop Poles for Example 1

Table *2.* Closed-Loop Poles for Example 2

Table 3. Closed-Loop Poles for Example 3

Figure 1 Block Diagram of the Closed-Loop System

Figure 2 Eigenvalue Magnitude and Angle Plots

Figure 3 Butterworth Configuration for Optimal Root Loci

Figure 4 Eigenvalue Plots for Example 1

Figure 5 Eigenvalue Plots for Example 2

Figure 6. Complete Eigenvalue Plots for Example 2

Figure 7 Eigenvalue Plots for Example 3

Table 1 Closed-Loop Poles **for** Example 1

i	$\lambda_i^{(1)}$	$\lambda_i^{(2)}$
1	14161+ *i*28272	4491.4 + / 8932.6
2	-14123-128296	-4453-18956.3
3	14161-/28272	4491.4-i8932.6
4	-14123 +1 28296	-4453 + i 8956.3
5	-99.901	-99.893
6	-2.8327 +1 1.2699	-2.8329 + *i* 1.2699
7	-2.8327 -1 1.2699	-2.8329-1 1.2699

Table 2. Closed-Loop Poles **for Example** 2

i	$\lambda_i^{(1)}$	$\lambda_i^{(2)}$
1	-19.83 + *i* 19.85	-35.27 + i 35.28
2	-19.83 -1 19.85	-35.27 - *i* 35.28
3	-4.286	-13.54
4	-1.003	-1.002

Table 3. Closed-Loop Poles for Example 3

i	$\lambda_i^{(1)}$	^(2)
1	46416	10000
2	-23208 + *i*40197	-5000 + i 8660
3	-23208-/40197	-5000-/8660

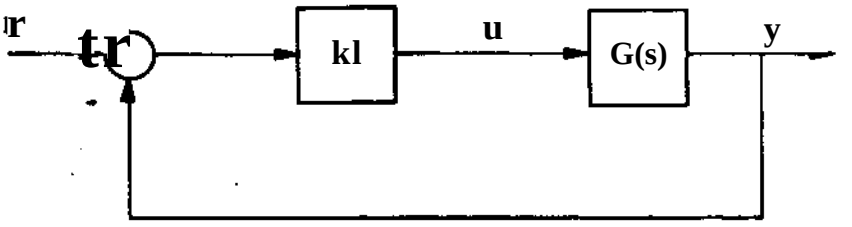

Figure 1 Block Diagram of the Closed-Loop System

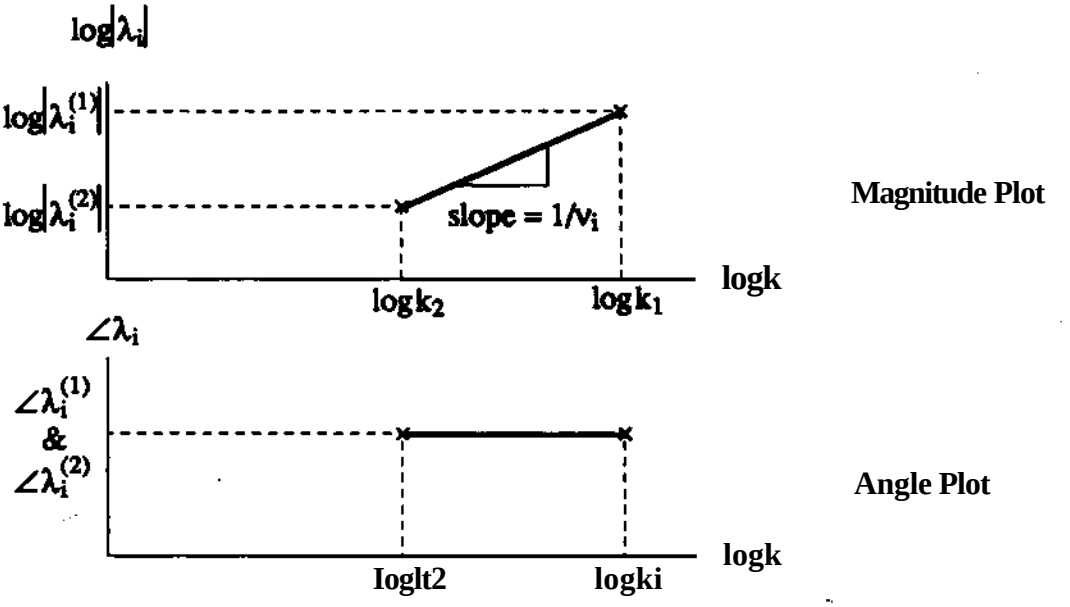

Figure 2 Eigenvalue Magnitude and Angle Plots

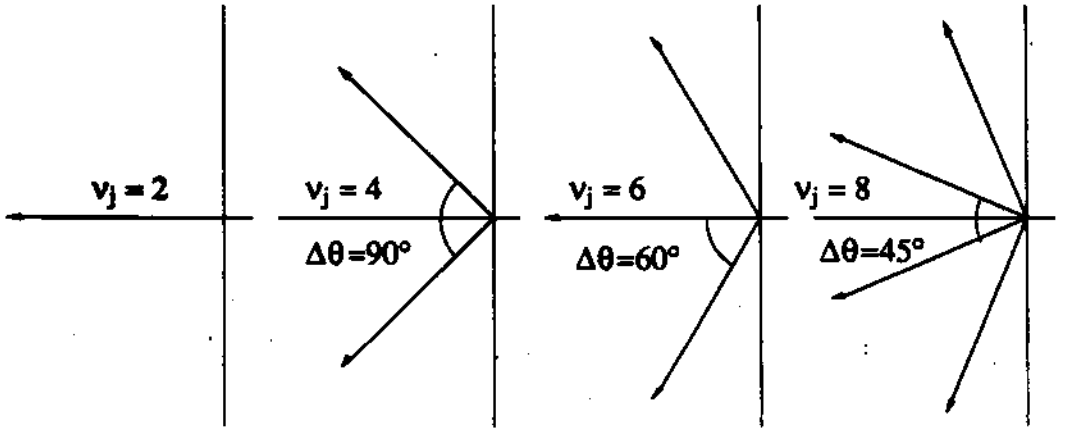

Figure 3 Butterworth Configuration for Optimal Root Loci

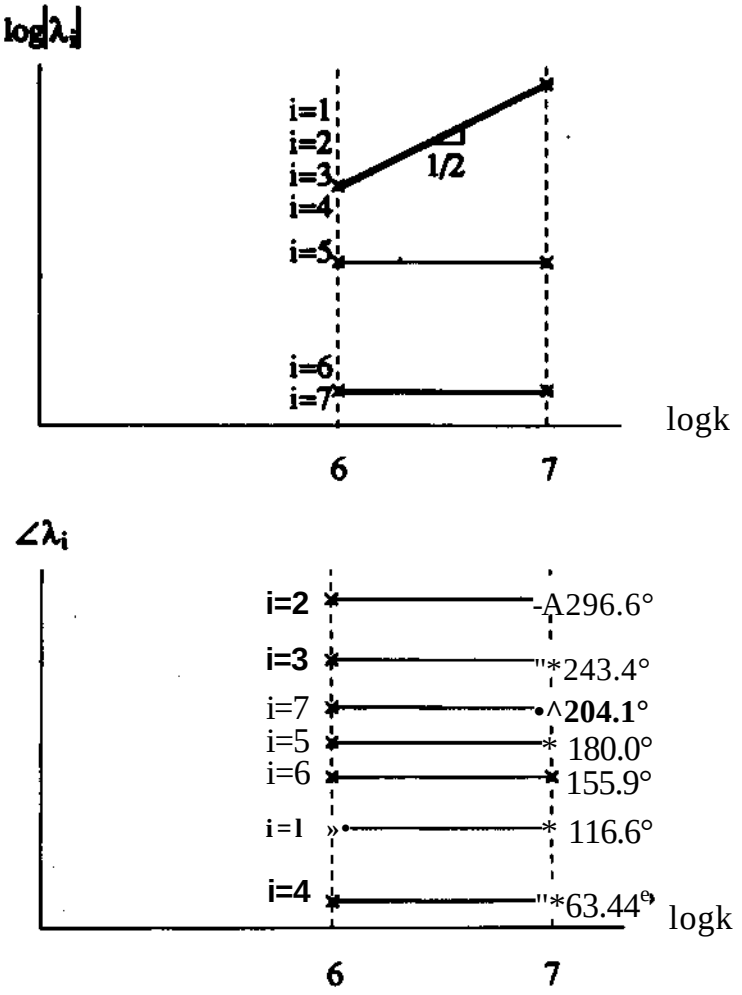

Figure 4 Eigenvalue Plots for Example 1

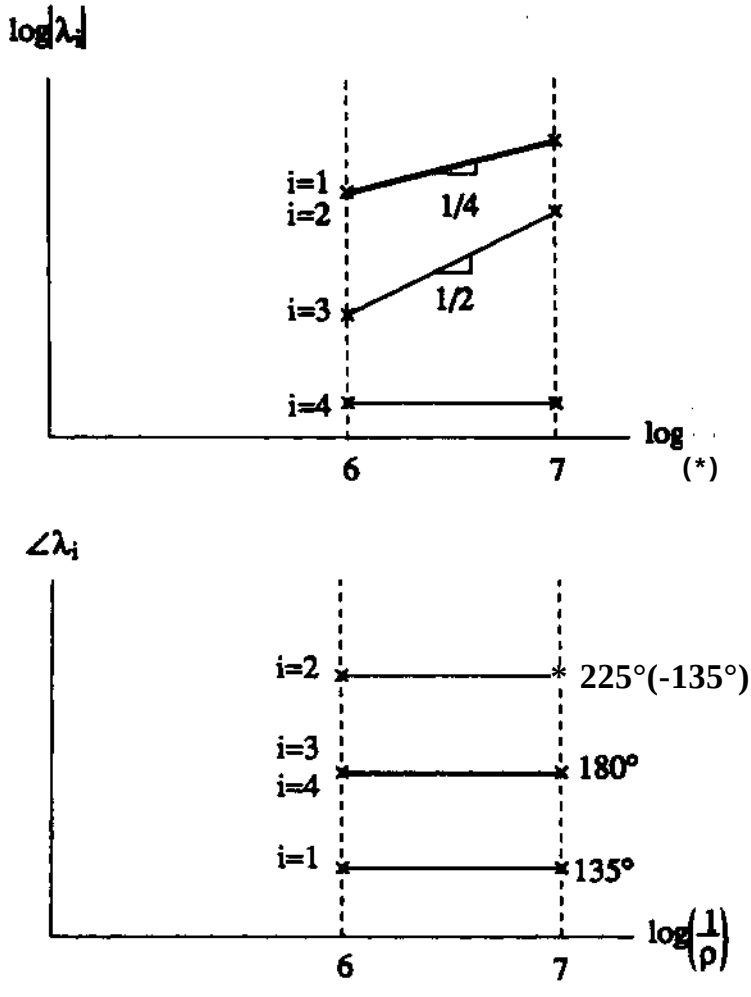

Figure 5 Eigenvalue Plots for Example 2

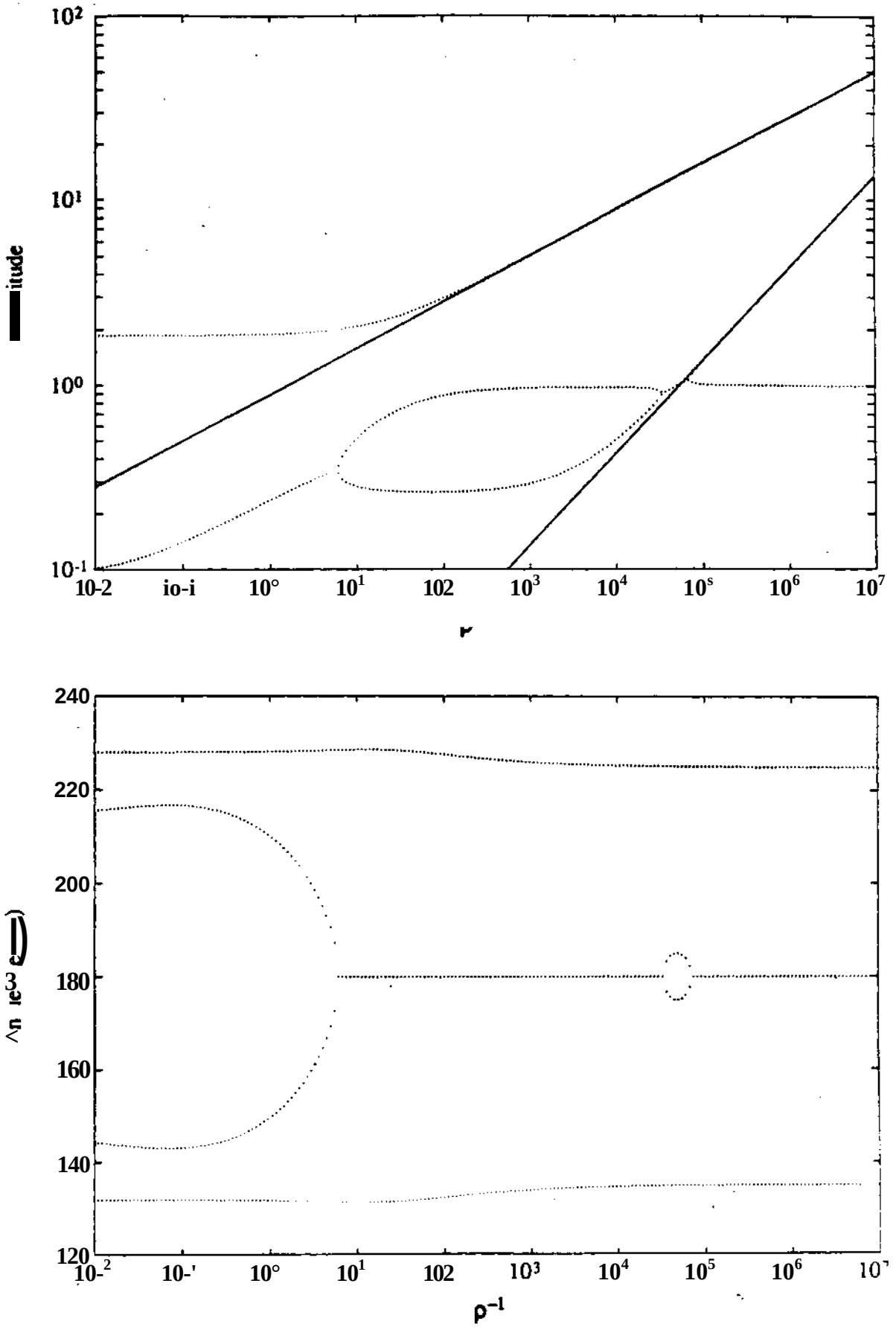

Figure 6. Complete Eigenvalue Plots for Example 2

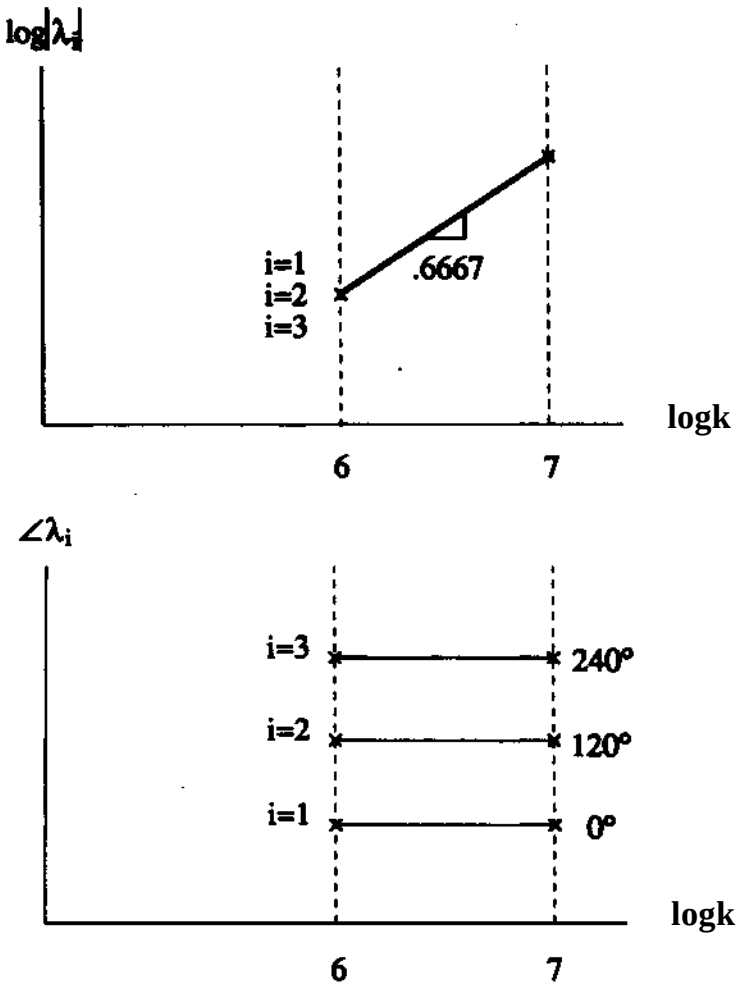

Figure 7 Eigenvalue Plots for Example 3